JOURNAL OF SOLID STATE CHEMISTRY 50, 121–128 (1983)

The Structures of the Lithium Inserted Metal Oxides $Li_{0.2}ReO_3$ and $Li_{0.36}WO_3$

R. J. CAVA, A. SANTORO,* D. W. MURPHY, S. M. ZAHURAK, AND R. S. ROTH*

*Bell Laboratories, Murray Hill, New Jersey 07974 and *U.S. Department of Commerce, National Bureau of Standards, Washington, D.C. 20234*

Received May 9, 1983; in revised form June 21, 1983

The crystal structure of $Li_{0.2}ReO_3$ has been determined and that of $Li_{0.36}WO_3$ redetermined by neutron diffraction powder profile analysis. The compounds are formed by the ambient temperature reactions of *n*-BuLi with WO_3 and LiI with ReO_3. The insertion of Li in both cases distorts the vacant perovskite-like cavities of the MO_3 hosts by inducing a movement of the oxygen atoms of about 0.4 Å. The resultant cavities are partially occupied by Li in square planar coordination, with lithium–oxygen distances of about 2.2 Å. Up to 0.75 Li/host metal could be accommodated in interstitial sites of that type, but in both cases the cubic phase becomes unstable before that extent of insertion can be attained. The results of $Li_{0.36}WO_3$ are in agreement with those of an earlier study.

Lithium can be inserted into the channels or cavities of many transition metal oxides at ambient temperature either through chemical or electrochemical means. The insertion compounds formed in this process are most often not the equilibrium phases and therefore cannot generally be synthesized by other means. We have been studying the crystal structures of lithium inserted metal oxides in order to better understand the insertion process through the characterization of the lithium–oxygen coordination geometries and the changes in the geometry of the host structures on the accommodation of additional ions. For ReO_3, whose cubic crystal structure consists of corner shared ReO_6 octahedra, three distinct phases form on Li insertion (*1*): Li_xReO_3: $0.0 \leq x \leq 0.35$, $x = 1.0$, and $1.8 \leq x \leq 2.0$. Our earlier neutron diffraction powder profile analysis (NDPPA) studies of $LiReO_3$ and Li_2ReO_3 showed that for both structures the host ReO_3 structure undergoes significant distortion, through an approximately 60° twist about ⟨111⟩, to accommodate lithium for compositions with Li/Re > 1. This twist converts the oxygen array from $\frac{3}{4}$ CCP to complete (distorted) HCP, transforms the dodecahedral cavity into two octahedral sites (occupied by Li), and changes the symmetry from cubic to rhombohedral. The low lithium content phase is cubic with an X-ray diffraction unit cell quite similar to that of ReO_3. Until recently we have been unable to synthesize this compound in sufficient purity to study its crystal structure via NDPPA. Electrochemical studies of small test cells of the form Li/$LiClO_4$, carbon/ReO_3 indicated that the cubic insertion phase forms at approximately 3.0 V (vs Li metal) and therefore could be synthesized in a pure form by reaction with

0022-4596/83 $3.00

LiI, which mimics potentiostatic discharge to 2.85 V.

Neutron powder data for the related bronze $Li_{0.36}WO_3$ have been reported (*2*, *3*), which clearly show a doubled unit cell caused by a tilting of the WO_6 octahedra. The data were insufficient, however, to locate the lithium, which was inferred to reside in a four coordinate square planar site in the center of the smaller of the cavities formed by the tilt. Because of this ambiquity and the relationship to Li_xReO_3 we have also redetermined the structure of this phase.

Experimental

$Li_{0.2}ReO_3$ was prepared from ReO_3 (Alfa Inorganics), purified by iodine transport in a 450–400°C gradient, by the room temperature reaction LiI + ReO_3 → $Li_{0.2}ReO_3$ + I_2. A 70-ml solution of LiI, 0.5 *M*, in acetonitrile was added to 10.4 g powdered ReO_3 in a pyrex vessel (under He) and stirred for several days. The solid product was washed in acetonitrile and the process of reaction with fresh LiI solution repeated (three times) until X-ray diffraction patterns showed the product to be single phase. Titration of the iodine formed in the reaction and flame emission analysis both determined the lithium stoichiometry to be $Li_{0.20}ReO_3$.

$Li_{0.36}WO_3$ was prepared from WO_3 (Alfa Inorganics) heated to 200°C to assure the absence of hydration products. The stoichiometry corresponding to that of the equilibrium high temperature phase was obtained by adding a stoichiometric quantity of *n*-butyl lithium (14.8 ml) to a fixed quantity of WO_3 (23.93 g) and stirring in a sealed pyrex vessel for 2 days. In reactions of this type, where the stoichiometry of the product is not determined by mixing the host oxide with an excess of *n*-BuLi (which would have resulted in a product of stoichiometry $Li_{0.67}WO_3$ (*3*)), multiple phase products are generally obtained due to the inhomogeneity of the reaction. The product was therefore homogenized by pressing into pellets and annealing *in vacuo* for 6 days at 600°C. Powder X-ray diffraction showed the resulting product to be single phase.

Neutron diffraction measurements were performed on the high resolution five counter powder diffractometer at the NBS Reactor, with neutrons of wavelength 1.5416(3) Å. The experimental conditions used to collect the data are presented in Table I. The powder profile refinement was performed using the Rietveld program (*4*) adapted to the 5 detector diffractometer de-

TABLE I

EXPERIMENTAL CONDITIONS USED TO COLLECT THE NEUTRON POWDER INTENSITY DATA FOR $Li_{0.2}ReO_3$ AND $Li_{0.36}WO_3$

	Monochromatic beam
Wavelength:	1.5416(3) Å
Horizontal divergences:	
(a) in-pile collimator:	10′ arc;
(b) monochromatic beam collimator:	20′ arc
(c) diffracted beam collimator:	10′ arc
Monochromator mosaic spread:	~15′ arc
Sample container:	vanadium can ~ 10 mm in diameter
Angular ranges scanned by each detector:	10–40, 30–60, 50–80, 70–100, 90–120
Angular step:	0.05°

sign and modified to allow the refinement of background intensity (*5*).

The high resolution diffractometer, when used with the experimental conditions described in Table I, gives Gaussian instrumental profiles over the entire 2θ angular range within a very good approximation. Although the peak profiles from $Li_{0.36}WO_3$ were described well by the standard Gaussian function, those from $Li_{0.2}ReO_3$ were not. We therefore employed for the refinement of $Li_{0.2}ReO_3$ the modification of the Rietveld program describing non-Gaussian profiles with the Pearson type VII distribution, which allows the line shape to be varied continuously from Gaussian to Lorentzian by changing one additional profile parameter (*6*).

The neutron scattering amplitudes employed were $b(Li) = -0.214$, $b(Re) = 0.92$, $b(W) = 0.48$, and $b(O) = 0.58$ ($\times 10^{-12}$ cm) (*7*). Initial lattice parameters were obtained by estimate from the positions of lines at high 2θ values. Approximate values of the background parameters were obtained at positions in the patterns free from diffraction effects. The background was assumed to be a straight line with finite slope and was refined separately for each counter. This description is quite adequate for the compounds studied and for the small angular interval scanned by each counter. In the refinement of the structural models, all structural, lattice, and profile parameters were refined simultaneously. Refinements were terminated when in two successive cycles the factor R_w (see Table III) varied by less than one part in a thousand. In the final refinements 15 profile and 7 structural parameters were varied.

Results

$Li_{0.2}ReO_3$

Inspection of the neutron diffraction pattern from the $Li_{0.2}ReO_3$ indicated the true unit cell to be twice the 3.7-Å cell derived from X-ray diffraction, and of a body centered cubic lattice type, and suggested that the structure of $Li_{0.2}ReO_3$ might be closely related to that of the high temperature equilibrium cubic lithium tungsten bronze $Li_{0.36}WO_3$ (*2*).

Starting structural parameters for the Re and O atoms in space group *Im*3 (No. 204) were set equal to those of W and O in $Li_{0.36}WO_3$, i.e., site 8*c* for Re at (0.25, 0.25, 0.25), and site 24*g* for O at (0, *y*, *z*) with $y \approx 0.20$ and $z \approx 0.29$. Initial refinements of the structure were performed without lithium, but all the temperature and positional parameters and the profile and lattice parameters were varied. This refinement gave the agreement factors $R_N = 6.80\%$, $R_p = 7.77\%$, $R_w = 10.49\%$, with an $R_E = 5.92\%$. Difference Fourier syntheses employing the observed and calculated structure factors extracted from the profile fit, clearly showed the Li atoms to occupy positions 6*b* at (0.5, 0, 0), where a large negative scattering anomaly was present. No other significant features were present in the map. Addition of 0.2 Li/Re, or an occupancy in site 6*b* of $0.2 \div 0.75 = 0.267$ Li and re-refinement of the structure resulted in a significant improvement in all the agreement factors, as shown in Table II. A difference Fourier synthesis of the final structural model showed no significant features. The observed and calculated neutron diffraction powder profile for $Li_{0.2}ReO_3$, and the difference profile, are presented in Fig. 1. The diffracted lineshape was somewhat different from Gaussian, and was best described by the Pearson type VII distribution with $m = 4$.

A projection of the structure of $Li_{0.2}ReO_3$ into the (001) plane is shown in Fig. 2. The figure shows the slightly irregular ReO_6 octahedra whose rotation distorts the normally vacant perovskite-like cavity. The rotations allow the inserted Li ions to occupy a 4 coordinate site with reasonable Li–O distances of about 2.2 Å. The undistorted

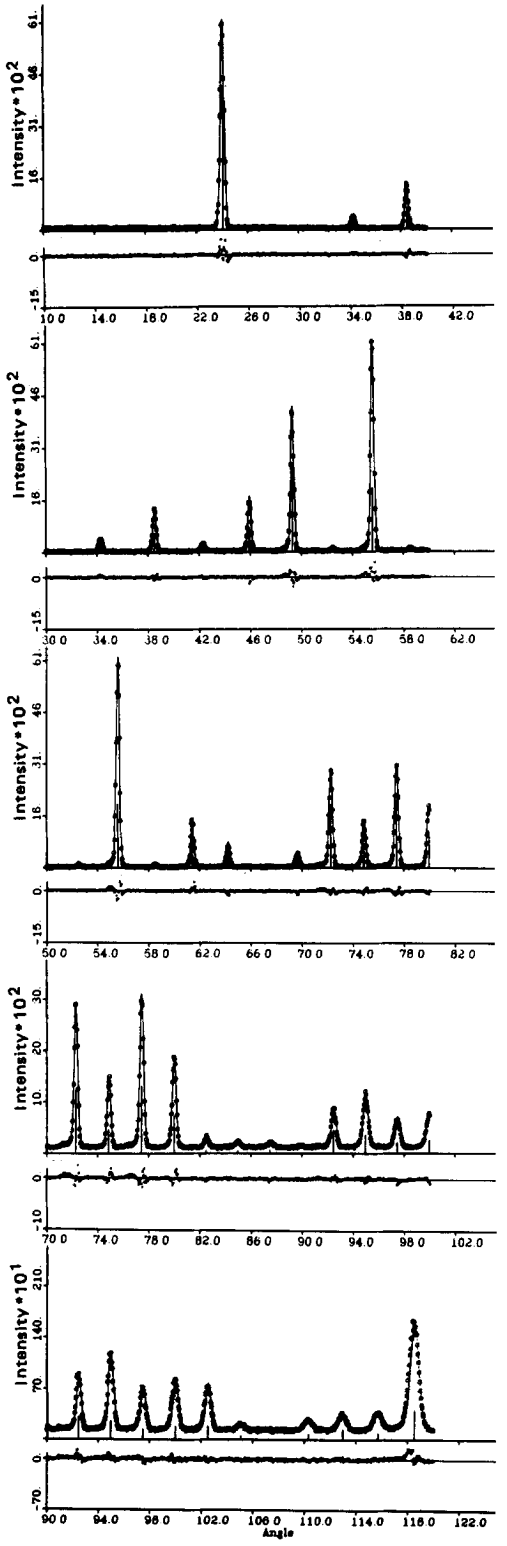

FIG. 1. Observed and calculated powder neutron diffraction profile intensities for $Li_{0.2}ReO_3$. Under the profile for each of the five detectors plotted on the same scale are the differences between the observed and calculated profiles.

TABLE II

LATTICE PARAMETERS, STRUCTURAL PARAMETERS, AND AGREEMENT FACTORS FOR $Li_{0.2}ReO_3$ AND $Li_{0.36}WO_3$ IN SPACE GROUP $Im3$

	$Li_{0.2}ReO_3$	$Li_{0.36}WO_3$
Lattice parameter		
a_0 (Å)	7.3979(1)	7.4529(1)
Structural parameters		
Lithium		
Position 6*b* (0.5, 0, 0)		
B (Å²)	1.5(4)	2.4(3)
Rhenium/tungsten		
Position 8*c* (0.25, 0.25, 0.25)		
B (Å²)	.15(2)	.39(4)
Oxygen		
Position 24*g* (0, *y*, *z*)		
y	.2133(2)	.2059(2)
z	.2844(3)	.2900(2)
B (Å²)	.76(2)	.86(2)
Agreement factors (%)		
R_N	4.29	4.93
R_p	6.89	6.96
R_w	9.64	9.23
R_E	5.92	5.06
Line shape	Gaussian	Pearson type VII, $m = 4$

$$R_N = \frac{\Sigma|I(\text{obs}) - I(\text{calc})|}{\Sigma I(\text{obs})}$$

$$R_p = \frac{\Sigma|y(\text{obs}) - y(\text{calc})|}{\Sigma y(\text{obs})}$$

$$R_w = \left\{\frac{\Sigma w[y(\text{obs}) - y(\text{calc})]^2}{\Sigma w[y(\text{obs})]^2}\right\}^{1/2}$$

$$R_E = \left\{\frac{N - P + C}{\Sigma w[y(\text{obs})]^2}\right\}^{1/2}$$

where N = number of independent observations, P = number of parameters, C = number of constraints, y = counts at angle 2θ, I = integrated Bragg intensities, and w = weights.

ReO_3 host has one perovskite cavity per Re atom (8 per 7.4-Å body centered cell) with a 12 coordinate center. The distortion occurring in $Li_{0.2}ReO_3$ creates cavities of two different geometries in the ratio (per unit cell) of 6 : 2 through displacements of the oxygen atoms of about 0.4 Å from their ReO_3 posi-

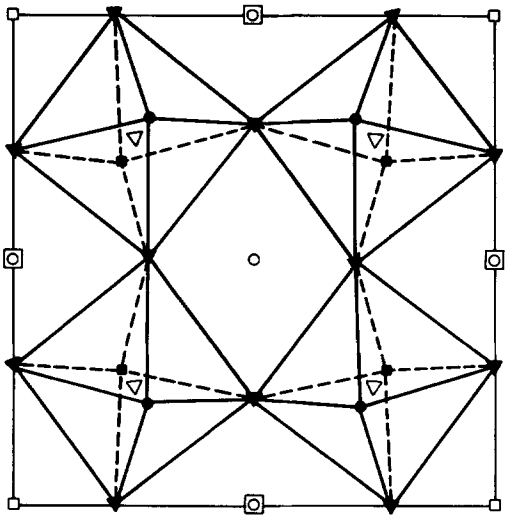

FIG. 2. The structure of $Li_{0.2}ReO_3$ projected into the (001) plane: ∇ = Re, $z = \frac{1}{4}$; $z = \frac{3}{4}$; ▼ = O, $z \approx \frac{1}{4}$; $z \approx \frac{3}{4}$; ● = O, $z \approx 0$, $z \approx 1$, ■ = O, $z \approx \frac{1}{2}$; ○ = Li, $z = 0$, $z = 1$; □ = Li, $z = \frac{1}{2}$. One plane of ReO_6 octahedra is outlined.

tions. The lithium occupy the more numerous (6*b*) sites in square planar coordination. The unoccupied cavities (2*a* sites) would have 12 coordinate Li–O distances of 2.63 Å and are thus too large for lithium occupancy.

Bond lengths and angles for the metal–oxygen coordination polyhedra are presented in Table III. The Re–O bond distance (1.887 Å) is only slightly larger than the Re–O distance in ReO_3 (1.874 Å), with the octahedron nearly perfectly regular. The Li–O square planar coordination is also quite regular, with metal–oxygen distances of 2.244(2) Å. There are four more oxygen atoms at approximately 2.65 Å. Also included in Table III are selected metal–metal distances.

$Li_{0.36}WO_3$

Starting structural parameters for the W and O atoms in space group *Im*3 (No. 204) were taken as those reported for $Li_{0.36}WO_3$ (W : 8*c* (0.25, 0.25, 0.25); O : 24*g*, (0, *y*, *z*) $y \approx 0.20$, $z \approx 0.29$). Initial refinements with Li omitted and all remaining structural and profile parameters varied converged to agreement factors (%) of $R_N = 9.70$, $R_p = 8.12$, $R_w = 10.44$, with an expected agreement $R_E = 5.06$. Difference Fourier synthesis employing the observed and calculated structure factors extracted from the profile fit clearly showed the Li positions to be 6*b* (0.5, 0, 0), by the presence of a large negative scattering anomaly, and showed no other significant features. Refinements with lithium located in the 6*b* site (occupancy = $0.36 \div 0.75 = 0.48$) resulted in significantly improved agreement factors, as shown in Table II. The improvement of the agreement factor for intensities, from 9.70 to 4.93%, indicates a much greater sensitivity of the data to the lithium positions than in an earlier study (*2*), where the agreement factor was unchanged by the addition of the lithium. Our final model is, however, essentially identical to that proposed previously,

TABLE III

BOND LENGTHS AND ANGLES FOR $Li_{0.2}ReO_3$ AND $Li_{0.36}WO_3$

	$Li_{0.2}ReO_3$	$Li_{0.36}WO_3$
Li polyhedron		
Li–O		
(×4)	2.244(2)	2.192(2)
O–Li–O		
(×2)	90.61(7)	91.13(8)
(×2)	89.39(7)	88.87(8)
O–O		
(×2)	3.156(3)	3.069(3)
(×2)	3.190(3)	3.130(3)
Re/W octahedron		
Re(W)–O		
(×6)	1.887(1)	1.915(1)
O–Re(W)–O		
(×6)	90.61(6)	90.64(6)
(×6)	89.39(6)	89.36(6)
O–O		
(×6)	2.652(2)	2.694(2)
(×6)	2.682(2)	2.724(2)
Metal–Metal		
Li–Li	3.699(1)	3.726(1)
Li–Re(W)	3.203(1)	3.227(1)
Re(W)–Re(W)	3.699(1)	3.726(1)

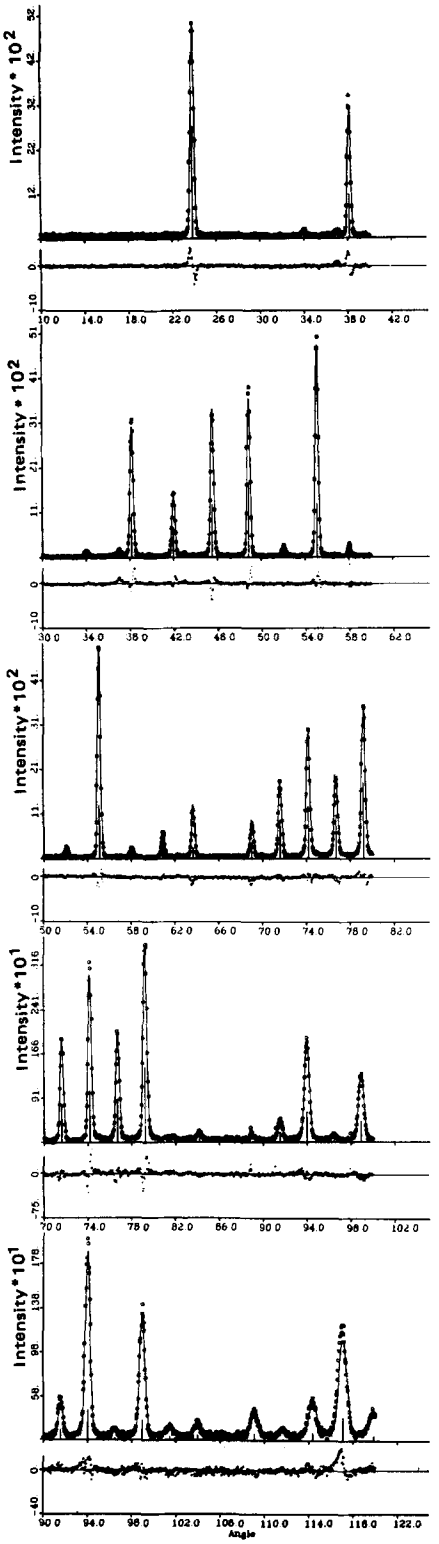

with our oxygen positions and those proposed earlier agreeing to within one or two standard deviations. Difference Fourier synthesis of the final structural model showed no significant features. The observed and calculated neutron diffraction powder profile for $Li_{0.36}WO_3$, and the difference profile, are presented in Fig. 3. The diffracted lineshape for this compound is best described by the standard Gaussian distribution.

As can be seen in the comparison of the entries in Table II, the structures of $Li_{0.2}ReO_3$ and $Li_{0.36}WO_3$ are identical except in some details. Bond lengths and angles for the metal–oxygen coordination polyhedra for $Li_{0.36}WO_3$ are presented in Table III. The Li–O square planar coordination is quite similar to that found in $Li_{0.2}ReO_3$, with Li–O distances of approximately 2.19 Å. Four more oxygen atoms can be found at approximately 2.69 Å. As in $Li_{0.2}ReO_3$, the eight perovskite-like cavities per unit cell in $Li_{0.36}WO_3$ are transformed by the distortion into a group of six (occupied) and a group of two (unoccupied). The unoccupied cavities have 12 coordinate centers with potential Li–O distances of 2.65 Å.

Discussion and Conclusions

The cubic ReO_3 and WO_3 host structures distort at low lithium insertion stoichiometries and give body centered cubic cells with doubled lattice parameter. The new cells allow $\frac{3}{4}$ of the perovskite cavities to accommodate lithium in 4 coordinate square planar sites with Li–O bond distances of approximately 2.2 Å. The distortion involves rotations of the MO_6 host octahedra that result in displacements of the

FIG. 3. Observed and calculated powder neutron diffraction profile intensities for $Li_{0.36}WO_3$. Under the profile for each of the five detectors, plotted on the same scale, are the differences between the observed and calculated profiles.

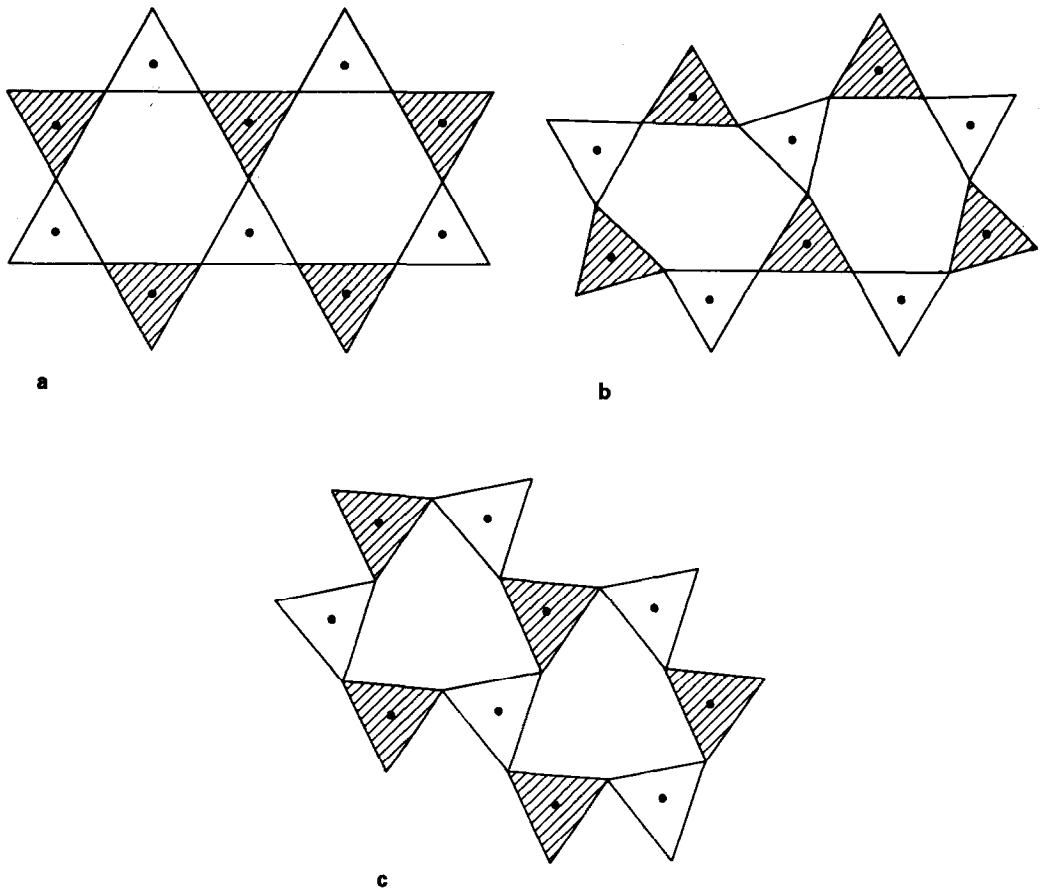

FIG. 4. The relation between ReO_3, $Li_{0.2}ReO_3$, and $LiReO_3$ viewed in the cubic (111) and hexagonal (001) planes. Cations for the ReO_3 host structure shown as solid circles and the triangles are the triangular faces of the ReO_6 octahedra sharing corners (oxygen atoms are at the vertices). Shaded triangles are associated with octahedra above the plane of the figure, and unshaded triangles, octahedra below. (a) ReO_3; (b) $Li_{0.2}ReO_3$; (c) $LiReO_3$.

oxygen atoms of approximately 0.4 Å from their ideal MO_3 positions. If all of the potential 4 coordinate sites were to be filled, inserted stoichiometries of $Li_{0.75}MO_3$ would occur in the BCC phase. For both ReO_3 and WO_3, however, this lithium stoichiometry cannot be obtained without introducing more severe distortions: the stoichiometry limits for the cubic phases are approximately $Li_{0.35}ReO_3$ and $Li_{0.67}WO_3$ (*1*, *3*). For the Li_xReO_3 case the distortion at high lithium insertion stoichiometries results in an HCP $LiNbO_3$-like structure, whereas in Li_xWO_3 the distortion has not been characterized. Inspection of the reported powder pattern for $Li_{2.5}WO_3$ (*3*) does not reveal an obvious relation to the HCP Li_xReO_3 phases.

For values of $x \geq 1$ in Li_xReO_3, the ReO_3 host structure undergoes a distortion which can be described by a twist of approximately 60° about one ⟨111⟩ direction. A projection of the host structure of $Li_{0.2}ReO_3$ down ⟨111⟩ is shown in Fig. 4. The figure shows the triangular faces of the MO_6 octahedra in one (111) plane for (a) the undis-

torted $\frac{3}{4}$ CCP ReO_3 structure, (b) the distorted $\frac{3}{4}$ CCP $Li_{0.2}ReO_3$ structure, and (c) the distorted HCP $LiReO_3$ structure. For $LiReO_3$ and ReO_3, oxygen atoms are coplanar, but for $Li_{0.2}ReO_3$ the oxygen atoms deviate ± 0.3 Å from the (111) planes. The figure illustrates the significant distortion of $\frac{3}{4}$ of the perovskite-like cavities in $Li_{0.2}ReO_3$, but shows also that the distortion is not well described simply as a ⟨111⟩ twist.

The square planar lithium–oxygen coordination in $Li_{0.2}ReO_3$ and $Li_{0.36}WO_3$ is somewhat unusual in oxides, and is no doubt a compromise to accommodate Li in sites of the available geometry. The Li–O bond distances of approximately 2.2 Å are somewhat larger than that usually observed for octahedral or tetrahedral coordination (approximately 2.0 Å) in oxides, and are very similar to those we have observed for 5 coordinate Li in the insertion compound $Li_2FeV_3O_8$ (*8*).

Lithium insertion reactions have been observed for many compounds whose host structure is derived by crystallographic shear (*CS*) of the ReO_3 type structure. In these *CS* structures, in general, the perovskite-like cavities are capped by additional oxygen atoms, providing interstititial sites of at least fivefold coordination. In many cases, however, Li atoms are probably accommodated in noncapped perovskite cavities. In the *CS* structures, extensive distortion of such cavities is prevented by edge sharing of the MO_6 host octahedra, and thus distortions of the type observed in $Li_{0.2}ReO_3$ and $Li_{0.36}WO_3$ probably do not occur. It would be of interest to determine the coordination geometry of inserted lithium in the perovskite-like cavities of such rigid *CS* structures.

References

1. R. J. Cava, A. Santoro, D. W. Murphy, S. M. Zahurak, and R. S. Roth, *J. Solid State Chem.* **42,** 251 (1982).
2. P. J. Wiseman and P. G. Dickens, *J. Solid State Chem.* **17,** 91 (1976).
3. K. H. Cheng and M. S. Whittingham, *Solid State Ionics* **1,** 151 (1980).
4. H. M. Rietveld, *J. Appl. Crystallogr.* **2,** 65 (1969).
5. E. Prince, "U. D. Tech. Note 1117" (F. J. Shorten, Ed.), p. 8–9, Nat. Bureau of Standards, Washington, D. C., 1980.
6. A. Santoro, R. J. Cava, D. W. Murphy, and R. S. Roth, "Neutron Scattering" (J. Faber, Ed.), p. 162, Conference Proceedings 89, American Institute of Physics, 1982.
7. G. E. Bacon, *Acta Crystallogr. Sect. A* **28,** 357 (1972).
8. R. J. Cava, A. Santoro, D. W. Murphy, S. M. Zahurak, and R. S. Roth, *J. Solid State Chem.*, in press.